Journal of Alloys and Compounds 509 (2011) 2976–2980

Contents lists available at ScienceDirect

Journal of Alloys and Compounds

journal homepage: www.elsevier.com/locate/jallcom

Effects of lanthanum doping on the preferred orientation, phase structure and electrical properties of sol–gel derived $Pb_{1-3x/2}La_x(Zr_{0.6}Ti_{0.4})O_3$ thin films

S.Q. Zhang, L.D. Wang, W.L. Li, N. Li, W.D. Fei*

Stake Key Laboratory of Advance Welding Production Technology, School of Materials Science and Engineering, Harbin Institute of Technology, Harbin 150001, PR China

ARTICLE INFO

Article history:
Received 18 August 2010
Received in revised form
24 November 2010
Accepted 25 November 2010
Available online 3 December 2010

Keywords:
Thin film
Sol–gel processes
X-ray diffraction
Microstructure
Electrical properties

ABSTRACT

$Pb_{1-3x/2}La_x(Zr_{0.6}Ti_{0.4})O_3$ thin films ($0 \le x \le 0.08$) were prepared on the Pt (1 1 1)/Ti/SiO_2/Si (1 0 0) substrates by a sol–gel method. The morphology, preferred orientation, phase structure, dielectric and ferroelectric properties of the films have been investigated. Our results show that lanthanum doping is favorable to enhance crystalline and obtain (1 0 0)-preferred orientation of the films. Meanwhile, it is suggested that the films undergo a structure change from "rhombohedral" phase to monoclinic phase as the lanthanum-doped content is increased to $x \approx 0.05$. Results of dielectric properties and ferroelectric properties indicate that lanthanum doping contributes to improve film dielectric constant and dielectric loss while it brings about a striking decrease in remnant polarization value. Possible explanations for the variations of electrical properties have been discussed in terms of preferred orientation, phase structure and large lattice distortion.

1. Introduction

Polycrystalline La-doped PZT (PLZT) thin film is an excellent candidate material for multifunctional optoelectronic devices due to its high electro-optical coefficient, fast response time and memory capability [1–3]. The addition of donor dopants such as La^{3+} cation is an effective way in reducing the leakage current and improving the fatigue behavior of PZT thin films due to its role in diluting oxygen vacancy concentrations [4–7]. Studies also indicated that La doping could greatly tailor the electrical properties of PZT bulk ceramics and similar perovskite oxides [8–10]. In order to optimize the performance of thin films, it is essential to understand those factors that may influence the properties of ferroelectric thin films. Our previous studies have shown that the polarization behavior of polycrystalline PZT thin films greatly depends on preferred orientation, monoclinic phase and associated residual stress [11–13]. For example, the 300 nm thick $Pb(Zr_{0.52}Ti_{0.48})O_3$ film exhibits higher remnant polarization value than that of the 200 nm thick PZT film [12]. Especially, it is suggested that residual stress status is tensile for the (1 0 0)-oriented thin films and is compressive for the (1 1 1)-oriented thin films [13]. For ferroelectric PLZT thin films, some researchers have investigated the influences of La-doped contents and substrates on the microstructure and electrical properties [14–18]. The loss tangent of PLZT thin film can be decreased while the remnant polarization value increased by La doping due to the combined effects of enhanced domain wall motion and stabilized tetragonal phase [18]. However, the preferred orientation, phase structure and electrical properties of PLZT thin films have not been reported until now. Therefore, the objective of our work is to investigate the effects of La doping on the microstructure and electrical properties of Zr-rich PLZT(x/60/40) thin films with a Zr/Ti ratio of 60/40. A variety of techniques including MOCVD, sputtering and sol–gel process have been developed to fabricate ferroelectric thin films. Among these techniques, the sol–gel process has attracted increasing attention because of its chemical homogeneity and facility of stoichiometry control [19], which is promising for producing dense microstructures.

2. Experimental procedures

The sol–gel method was used to prepare the films on the Pt (1 1 1)/Ti/SiO_2/Si (1 0 0) substrates, which has been described in detail elsewhere [11]. The concentration of the $(Pb_{1-3x/2}La_x)(Zr_{0.6}Ti_{0.4})O_3$ precursors ($0 \le x \le 0.08$) was all adjusted to 0.3 M. Each layer was spin-coated on the substrate at 3000 rpm for 15 s, and then the wet film was dried on a hot plate at 425 °C for 3 min. By repeating the above processes several times, the wet films with a desired thickness (~350 nm) were obtained. Then, these films were annealed by rapid thermal annealing (RTA) furnace at 650 °C for 5 min in an oxygen atmosphere. The crystal structures of the films were characterized using a Philips' X-ray diffractometer (XRD) with Cu Kα radiation at 40 kV and 40 mA. Gold top electrodes of around 0.2 mm in diameter were deposited on the films through a shadow mask in a vacuum evaporation system. The polarizations versus electric field loops were measured using a ferroelectric test system (P-LC100, Radiant Technology). The dielectric properties of the films were obtained by HP 4294 impedance analyzer with the frequency ranging from 100 Hz to 1 MHz and AC signal amplitude of 500 mV.

* Corresponding author.
E-mail address: wdfei@hit.edu.cn (W.D. Fei).

0925-8388/$ – see front matter © 2010 Elsevier B.V. All rights reserved.
doi:10.1016/j.jallcom.2010.11.177

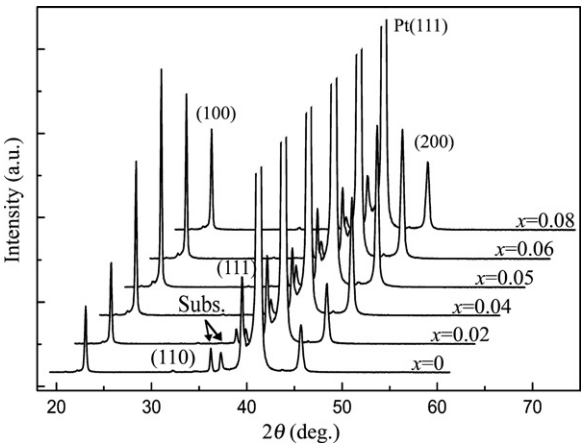

Fig. 1. XRD patterns of the films.

3. Results and discussion

3.1. Preferred orientation of the films

Fig. 1 shows the XRD patterns of the films. As can be seen, all the films crystallize in single perovskite phase without unwanted pyrochlore phase and have a mixture of (1 0 0) and (1 1 1) preferred orientations. Compared with the intensity of (1 1 1) reflection, a relative lower intensity of (1 0 0)/(2 0 0) reflections suggests that the PZT film undoped has a dominant (1 1 1)-preferred orientation. However, it is found that with the increase of x, the films tend to have a decreasing intensity of (1 1 1) reflection and an increasing intensity of (1 0 0) reflection. In addition, the intensity of (1 1 0) reflection is very weak for all the films. The preferential orientations can be quantitatively expressed through the orientation degree as follows,

$$\alpha_{(100)} = \frac{I_{(100)}}{I_{(111)} + I_{(100)} + I_{(110)}} \times 100\%,$$

where $I_{(hkl)}$ is the integrated intensity of the corresponding diffraction peaks. Fig. 2 shows the α_{100} value dependence on the La-doped content. As seen in Fig. 2, with the increase of x ($0 \le x \le 0.05$), α_{100} value increases from 30% to 60% although it then begins to decrease. Thus, the results suggest that La doping contributes to higher (1 0 0)-preferred orientation. A decreased α_{100} value for $x \ge 0.06$ may be associated with some changes of surface morphology and higher lead deficiency.

The formation mechanisms of preferred orientations in PZT thin films have been investigated by some researchers [20,21]. Generally, it is believed that PZT thin films tend to take (1 1 1) preferred orientation on the (1 1 1)-oriented Pt substrates due to the lattice matching effect and the presence of an inter-metallic phase $Pt_{5-7}Pb$ in the early stage of the crystallization. While the presence of (0 0 1)-oriented PbO buffer layer at an appropriate process parameters favors the nucleation of (1 0 0)-oriented PZT. Now that all the films are prepared under the same thermal treatment condition, the mechanism of PbO buffer layer cannot be used to explain the phenomenon of an increasing (1 0 0) orientation degree observed in the films. Higher (1 0 0)-preferred orientation means that the nucleation of the PLZT films is weakly controlled by the substrate effect. Considering a smaller ionic radius of La^{3+} (1.21 Å) as compared with Pb^{2+} (1.15 Å) [22], the enhancement of (1 0 0)-preferred orientation in the films within certain La-doped content region may result from an enlarged lattice mismatching between the films and the substrates.

Fig. 3 shows the surface morphology of the films characterized by SPM (SPI4000&SPA300HV, Seiko) using an atomic force microscopy (AFM) mode. All images were achieved with length within 500 nm × 500 nm at room temperature. It can be seen that the surfaces are smooth, dense and uniform without any rosette structure, which suggests that all the films are of good qualities. The average grain sizes of the films were estimated directly from AFM. In Fig. 3(a) and (b), the films have fine grain sizes (around 27 nm in average). In contrast, it is observed from Fig. 3(c) and (d) that the films with higher x values have relative large grain sizes (around 37 nm in average), which indicates a beginning of the coalescence process.

3.2. Phase structure of the films

Fig. 4 gives the observed and calculated profiles of $(2\,0\,0)_{pc}$ reflections of the films in a pseudocubic coordinate system. During the peak-fitting procedure, a Pseudo-Voigt2 function was used to define the profile shapes while background was estimated by linear interpolation between fixed values. It is observed from Fig. 4(a)–(c) that the profiles of $(2\,0\,0)_{pc}$ reflections are symmetry for $x \le 0.04$. In contrast, the profiles of $(2\,0\,0)_{pc}$ reflections for $x \ge 0.05$ are asym-

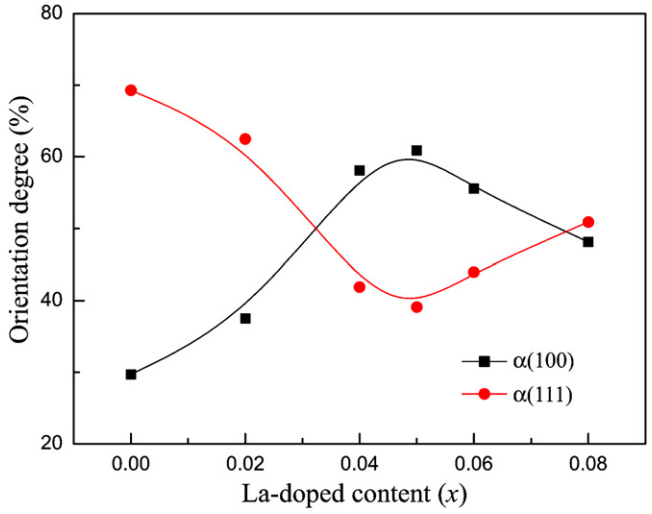

Fig. 2. Calculated (1 1 1) and (1 0 0) orientation degree of the films as a function of La-doped content.

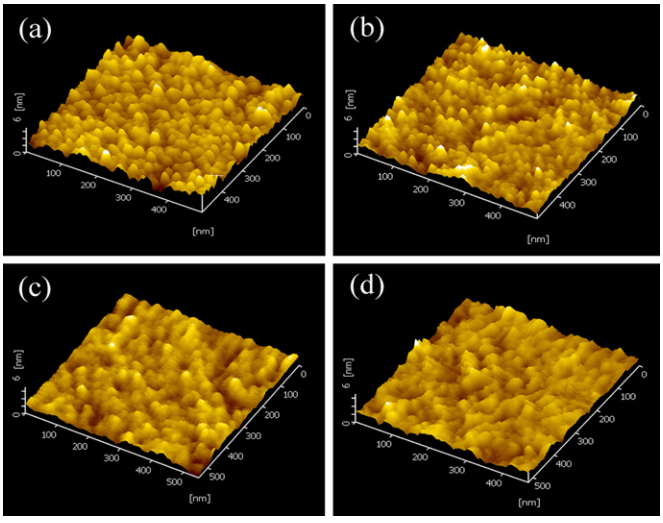

Fig. 3. Atomic force microscopy images of the films with (a) $x = 0$, (b) $x = 0.04$, (c) $x = 0.06$ and (d) $x = 0.08$, respectively.

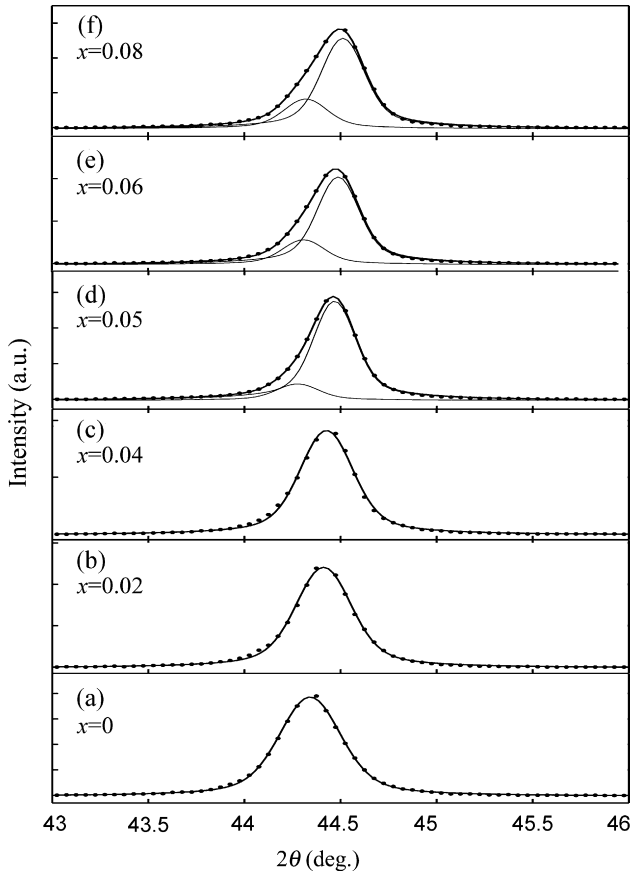

Fig. 4. Observed and calculated profiles of $(2\,0\,0)_{pc}$ reflections of the films using pure rhombohedral phase mode for $x \leq 0.04$ and monoclinic phase (*Cm*) model for $0.05 \leq x \leq 0.08$.

metric obviously, as shown in Fig. 4(d)–(f). It is also observed that the position of $(2\,0\,0)_{pc}$ reflections tends to be shifted toward high 2θ angle (~44.5°), which is expected considering the replacement of Pb^{2+} with the smaller ionic radius of La^{3+} at A site. In addition, a reduction of oxygen vacancies concentration in PLZT thin films also provokes the decrease of *a*-axis lattice parameter [23]. For the rhombohedral phase of PZT (*R*3*m* space group), it is well established that the profile of $(2\,0\,0)_{pc}$ reflection is a singlet whereas the profiles of $(2\,0\,0)_{pc}$ reflections for the tetragonal and monoclinic phase (*Cm* space group) are doublet. Following this, the structure for $x \leq 0.04$ is "rhombohedral" as the $(2\,0\,0)_{pc}$ reflection is a symmetry singlet. However, with the increase of *x*, an asymmetric $(2\,0\,0)_{pc}$ reflection for $x \geq 0.05$ clearly indicates that the phase structure is not anymore "rhombohedral" but other possible phases (monoclinic or tetragonal phases). Here, it should be noted that such "rhombohedral" phase cannot be unquestionably taken as rhombohedral phase. Recently, some hitherto believed rhombohedral compositions of PZT including a Zr/Ti ratio of 60/40 are proposed to be monoclinic phase [24]. Because both phases exhibit similar characteristics observed in these literatures, it is quite difficult for us to distinguish monoclinic phase from rhombohedral phase. So we call this phase as "rhombohedral" phase for $x \leq$ 0.04. A fine scan XRD on $(1\,1\,1)_{pc}$ reflection (around 38.2°, $\psi = 55°$) of the films was also carried out to provide a further information. All the films exhibit an asymmetric profile of $(1\,1\,1)_{pc}$ reflection with a lower left shoulder, which not only supports the proposed "rhombohedral" phase for $x \leq 0.04$ but also clearly rules out the probability of tetragonal phase for $x \geq 0.05$. Here, we consider that the structure for $x \geq 0.05$ might be monoclinic phase (*Cm* space group) if

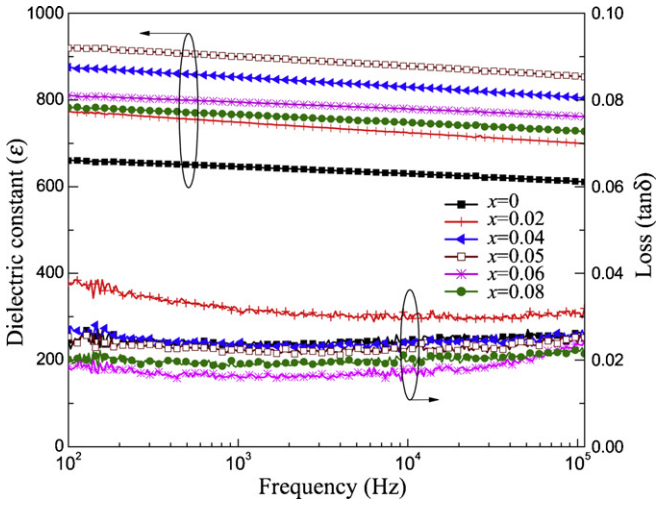

Fig. 5. Dielectric constant and loss tangent of the films.

some important literatures related to Pb-based perovskite ferroelectrics are fully taken into consideration. In the phase diagram of PZT, since an intermediate monoclinic phase (*Cm* space group) was discovered in PZT [25], rhombohedral phase coexisting with tetragonal phase near the morphotropic phase boundary (MPB) has been widely debated. Subsequently, a series of monoclinic phases (M_A, M_B, M_C) are discovered between rhombohedral and tetragonal phase in Pb-based perovskite ferroelectrics such as PZT [26], PZN-PT [27,28], and PMN-PT [29,30]. In the present study, it is suggested that the PLZT films undergo a structure change from "rhombohedral" phase to monoclinic phase as the La-doped content is increased to $x \approx 0.05$.

3.3. Dielectric properties and ferroelectric of the films

Fig. 5 shows the dielectric constant (ε) and the dielectric loss ($\tan\delta$) of the films measured at room temperature. It can be seen from Fig. 5 that ε and $\tan\delta$ values are greatly affected by La doping. With the increase of *x*, ε value reaches its maximum at $x = 0.05$ where the phase transition from rhombohedral and monoclinic phase occurs, and then it begins to decrease. Roughly, the films have decreasing $\tan\delta$ values except for an abnormal high $\tan\delta$ value at $x = 0.02$. The ε values of the films with *x* ranging from 0 to 0.08 are around 629, 724, 829, 878, 780, and 748 at 10 kHz, respectively. The corresponding $\tan\delta$ values are around 0.024, 0.029, 0.024, 0.023, 0.017, and 0.019, respectively. In the present study, a slight composition difference corresponding to dielectric maximum and loss tangent minimum is observed and the reasons for it are unclear. It might be resulted from their different temperature dependences of ε and $\tan\delta$ properties on the La-doped content [31]. For the films with *x* values ranging from 0 to 0.05, the dependences of dielectric properties on the La-doped content can be mainly explained by the fact that donor doping like La^{3+} in the place of Pb^{2+} is an effective way to reduce the concentration of intrinsic oxygen vacancies and compensate the holes formed due to lead vacancies [4,7]. A reduce of oxygen vacancies in the lattice makes domain wall motion easier, and thus reduced $\tan\delta$ and increased ε values are obtained. In contrast, the decrease of ε values for the films with higher *x* values may be attributed either to the formation of a kind of bond paraelectric materials mostly distributing in the grain boundaries [32].

Fig. 6(a) demonstrates typical *P*–*E* hysteresis loops of the films measured at a frequency of 1000 Hz and an applied voltage of 18 V. It is observed that the PZT film exhibits well-defined hysteresis loop in contrast with that of the PLZT films. With the increase of *x*, hysteresis loop tends to become slimmer and more unsatu-

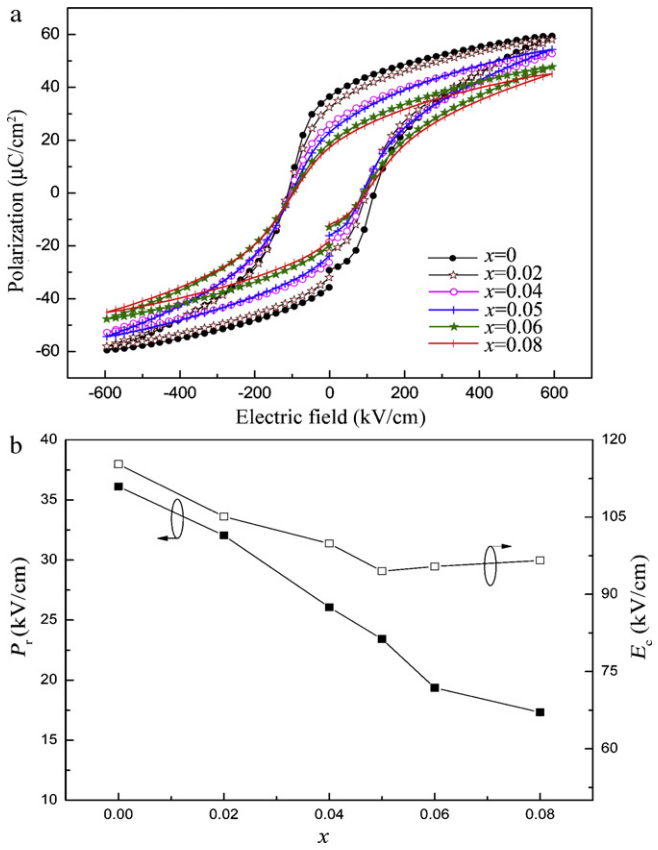

Fig. 6. (a) Typical *P*–*E* hysteresis loops of the films, and (b) Remnant polarization and coercive field of the films as a function of La-doped content.

rated. The dependence of remnant polarization (P_r) and coercive field (E_c) on the La-doped content is also given in Fig. 6(b). The P_r value of the films is strikingly reduced by the increment of La doping whereas the E_c value is reduced. The P_r values of the films with x values ranging from 0 to 0.08 are 36, 32, 26, 23, 19 and 17 μC/cm^2, respectively. The P_r value at $x = 0.08$ (~17 μC/cm^2) is comparable with those reported by Singh et al. [16,33] for PLZT (0.08/60/40) thin films prepared by sol–gel (~11.0 μC/cm^2) and RF sputtering (~15 μC/cm^2) methods. These P_r values are also similar to those reported by Park et al. [34] for PLZT (x/52/48) prepared by PMOD method (31 μC/cm^2 at $x = 0$ and 9 μC/cm^2 at $x = 0.05$). In contrast, these values are higher than those reported by Thomas et al. [35] for sol–gel-derived PLZT (x/65/35) thin films (16 μC/cm^2 at $x = 0$ and 6 μC/cm^2 at $x = 0.08$). The difference of P_r values for the same composition can be attributed to their different synthesis processes, substrate condition, preferred orientations as well as phase structures.

Until to now, the exact mechanism responsible for the electrical properties of ferroelectric thin films has not been well established. Generally, ferroelectric properties of thin films depend on the stress state and domain structure [36], as well as crystallographic orientation, phase and microstructure [37,38]. In Fig. 6(b), the variation of P_r value as a function of La-doped content can be explained by the conjoint contributions of the crystallographic orientation, phase structure and large lattice distortion. For the rhombohedral phase, because [1 1 1] is the polarization direction, the (1 1 1)-oriented films always have larger remnant polarizations as well as higher coercive fields than those of (1 0 0)-oriented films [39]. In contrast, the (1 0 0)-oriented films with tetragonal/monoclinic phase are expected to have higher P_r values. Following this, an increasing (1 0 0) preferred orientation degree for the films before $x = 0.05$ may contribute to the decrease of P_r values. However, for the films with monoclinic phase, an increasing (1 1 1) preferred orientation degree as well as the difficulty of 90° domain switching may result in the gradual decrease of P_r values. In addition, it is also suggested that large lattice distortion due to the addition of La doping may also play roles in reducing the P_r values of the films.

4. Conclusions

$Pb_{1-3x/2}La_x(Zr_{0.6}Ti_{0.4})O_3$ thin films ($0 \le x \le 0.08$) were prepared on the Pt (1 1 1)/Ti/SiO_2/Si (1 0 0) substrates by a sol–gel method. Atomic force microscopy was used to confirm the quality of the films while XRD was used to analysis film preferred orientation as well as phase structure. All the films exhibit good qualities and have a mixture of (1 0 0)-preferred and (1 1 1)-preferred orientation. Our results indicate that with the increase of La-doped content, (1 0 0)-preferred orientation of the films can be greatly enhanced. It is suggested that the films undergo a phase change from "rhombohedral" phase to monoclinic phase as the La-doped content is increased to $x \approx 0.05$. Dielectric and ferroelectric properties of the films indicate that La doping effectively enhances the dielectric constant while reduces the remnant polarization values. Possible explanations for the ferroelectric properties are presented in terms of crystallographic orientation, phase structure and large lattice distortion.

Acknowledgment

We would like to express our gratitude to Excellent Youth Foundation of Heilongjiang Scientific Committee of PR China.

References

[1] Z.H. Du, T.S. Zhang, H.M. Shang, X.L. Chen, J. Ma, Solid State Phenom. 136 (2008) 67–74.
[2] K. Uchiyama, T. Shiosaki, T. Kosaka, A. Kasamatsu, M. Echizen, Ceram. Int. 34 (2008) 979–983.
[3] Ø. Nordseth, C.C. You, E. Folven, S. Gariglio, A. Sambri, J.M. Triscone, J.W. Reiner, C.H. Ahn, T. Tybell, J.K. Grepstad, Thin Solid Films 518 (2010) 5471–5477.
[4] Z. Zhang, P. Wu, K.P. Ong, L. Lu, C. Shu, Phys. Rev. B. 76 (2007) 125102.
[5] S.J. Kang, Y.H. Joung, J. Mater. Sci. 42 (2007) 7899–7905.
[6] M.T. Chentir, E. Bouyssou, L. Ventura, G. Guegan, C. Anceau, Ferroelectrics 362 (2008) 123–127.
[7] N.K. Karan, R. Thomas, S.P. Pavunny, J.J. Saavedra-Arias, N.M. Murari, R.S. Katiyar, J. Alloys Compd. 482 (2009) 253–255.
[8] S.K. Pandey, O.P. Thakur, D.K. Bhattacharya, C. Prakash, R. Chatterjee, J. Alloys Compd. 468 (2009) 356–359.
[9] X. Zeng, X.Y. He, W.X. Cheng, X.S. Zheng, P.Q. Qiu, J. Alloys Compd. 485 (2009) 843–847.
[10] S. Singh, P. Singh, O. Parkash, D. Kumar, J. Alloys Compd. 493 (2010) 522–528.
[11] S.Q. Zhang, W.D. Fei, W.L. Li, J.N. Wang, J. Alloys Compd. 487 (2009) 703–707.
[12] C.Q. Liu, W.L. Li, W.D. Fei, S.Q. Zhang, J.N. Wang, J. Alloys Compd. 493 (2010) 499–501.
[13] J.N. Wang, W.L. Li, B. Feng, C.Q. Liu, X.L. Li, Q. Sun, W.D. Fei, J. Alloys Compd. 506 (2010) 167–171.
[14] R. Singh, T.C. Goel, S. Chandra, Mater. Res. Bull. 43 (2008) 384–393.
[15] G. Leclerc, G. Poullain, C. Yaicle, R. Bouregba, A. Pautrat, Appl. Surf. Sci. 254 (2008) 3867–3872.
[16] R. Singh, T.C. Goel, S. Chandra, Mater. Chem. Phys. 110 (2008) 120–127.
[17] M. Narayanan, B. Ma, U. Balachandran, Mater. Lett. 64 (2010) 22–24.
[18] S.Q. Zhang, W.L. Li, N. Li, W.D. Fei, Physica B 405 (2010) 2585–2588.
[19] R.W. Schwartz, T.J. Boyle, S.J. Lockwood, M.B. Sinclair, D. Dimos, C.D. Buchheit, Integr. Ferroelectr. 7 (1995) 259–277.
[20] S.Y. Chen, Mater. Chem. Phys. 45 (1996) 159–162.
[21] S.Y. Chen, I.W. Chen, J. Am. Ceram. Soc. 81 (1998) 97–105.
[22] R.C. Evans, An Introduction to Crystal Chemistry, Second ed., Cambridge Univ., London, 1964.
[23] H.L. Cai, X.S. Wu, J. Gao, Chem. Phys. Lett. 467 (2009) 313–317.
[24] A.K. Singh, D. Pandey, S. Yoon, S. Baik, N. Shin, Appl. Phys. Lett. 91 (2007) 192904.
[25] B. Noheda, D.E. Cox, G. Shirane, J.A. Gonzalo, L.E. Cross, S.E. Park, Appl. Phys. Lett. 74 (1999) 2059–2061.
[26] B. Noheda, J.A. Gonzalo, L.E. Cross, R. Guo, S.E. Park, D.E. Cox, G. Shirane, Phys. Rev. B 61 (2000) 8687–8695.
[27] K. Ohwada, K. Hirota, P.W. Rehrig, P.M. Gehring, B. Noheda, Y. Fujii, S.E.E. Park, G. Shirane, J. Phys. Soc. Japan 70 (2001) 2778–2783.
[28] B. Noheda, Z. Zhong, D.E. Cox, G. Shirane, S.E. Park, P. Rehrig, Phys. Rev. B 65 (2002) 224101.

[29] B. Noheda, D.E. Cox, G. Shirane, J. Gao, Z.G. Ye, Phys. Rev. B 66 (2002) 054104.
[30] A.K. Singh, D. Pandey, Phys. Rev. B 67 (2003) 064102.
[31] K. Bouayad, S. Sayouri, T. Lamcharfil, M. Ezzejari, D. Mezzane, L. Hajji, A. El Ghazouali, M. Filalil, P. Dieudonne, M. Rhouta, Physica A 358 (2005) 175–183.
[32] B. Tang, H.Q. Fan, S.M. Ke, L.J. Liu, Mater. Sci. Eng. B 138 (2007) 205–209.
[33] R. Singh, S. Chandra, S. Sharma, A.K. Tripathi, T.C. Goel, IEEE Trans. Dielectr. Electr. Insul. 11 (2004) 264–270.
[34] H.H. Park, W.S. Kim, J.K. Yang, H.H. Park, R.H. Hill, Microelectron. Eng. 71 (2004) 215–220.
[35] R. Thomas, S. Mochizuki, T. Mihara, T. Ishida, T. Mihara, T. Ishida, Thin Solid Films 443 (2003) 14–22.
[36] S.T. Mckinstry, J.F. Shepard, J.L. Lacey, T. Su, G. Zavala, J. Fendler, Ferroelectrics 206 (1998) 381–392.
[37] S.Y. Chen, C.L. Sun, J. Appl. Phys. 90 (2001) 2970–2974.
[38] W. Gong, J.F. Li, X.C. Chu, Z.L. Gui, L.T. Li, J. Appl. Phys. 96 (2004) 590–595.
[39] N.B. Gharb, I. Fujii, E. Hong, S.T. Mckinstry, D.V. Taylor, D. Damjanovic, J. Electroceram. 19 (2007) 47–65.